Actual Sensing Sensitivity and SNR Measurement of Optical Tweezers Based on Coulomb Force Input

Jiaojiao WANG[1], Xingfan CHEN[1,2*], Shaochong ZHU[2], Zhenhai FU[2], Nan LI[1], and Huizhu HU[1,2]

[1]*State Key Laboratory of Modern Optical Instrumentation, College of Optical Science and Engineering, Zhejiang University, Hangzhou 310027, China*

[2]*Quantum Sensing Center, Zhejiang Lab, Hangzhou 310000, China*

[*]Corresponding author: Xingfan CHEN E-mail: mycotty@zju.edu.cn

Abstract: Sensing sensitivity is the key performance of optical tweezers. By adjusting the frequency and magnitude of an applied Coulomb force as an input of optical tweezers, we directly measured the sensitivity and signal-to-noise ratio (SNR) of a system and indirectly calculated the actual noise magnitude. Combined with an output filter, the relationship between the SNR and bandwidths was studied. We established the simulation model of a system using Simulink and simulated the relationship between the SNR and magnitude of the input forces and filter bandwidths. In addition, we built an experimental system to determine the relationship between the SNR and the magnitude of the input forces and filter bandwidths. The actual minimum detectable force was measured as 1.8275×10^{-17} N at a 1 Hz bandwidth. The experimental results were correlated with the simulation and theoretical results, confirming the effectiveness of the proposed method and demonstrating the high sensitivity of vacuum optical tweezers as mechanical sensors. We proposed a novel method of calibration and measurement of system sensing parameters by applying an actual force that was more direct and precise than the theoretical calculation method that requires accurate fitting parameters, such as the particle radius and density. This method can be employed to analyze the system noise and phase characteristics to confirm and improve the real performance of the system.

Keywords: Optical tweezers; sensitivity; Coulomb force; SNR; Simulink; system noise characteristic

Citation: Jiaojiao WANG, Xingfan CHEN, Shaochong ZHU, Zhenhai FU, Nan LI, and Huizhu HU, "Actual Sensing Sensitivity and SNR Measurement of Optical Tweezers Based on Coulomb Force Input," *Photonic Sensors*, 2023, 13(1): 230124.

1. Introduction

The weak-force measurement is required in many fields, such as cell and tissue biological force studies; cell membrane elasticity measurements; production of gravimeters, accelerometers, and gyroscopes; detection of cosmic dark matter. The Casimir force and non-Newtonian gravity are particularly popular in extremely weak-force measurements. The Casimir force in quantum electrodynamics is a macroscopic phenomenon of the quantum effect, which requires consideration in the design of devices below the micron scale. The detection of the non-Newtonian gravity is also an arduous research project. In these studies, the force measurement with the high sensitivity is fundamental. Presently, the methods for measuring the weak force mainly include the torsion balance experiments, superconductivity technology, and optical-tweezer technology. In 1798, Cavendish

Received: 9 February 2022 / Revised: 5 June 2022

DOI: 10.1007/s13320-022-0665-6
Article type: Regular

employed torsion balance with his design, using a mirror and an extremely good and tough steel wire. He magnified the effects of the extremely weak gravity as observable quantities and created a new era of weak-force measurements. Scientists have continuously improved it for more precise weak-force measurements based on the experiment [1–5], which could reach the order of 10^{-9} N. The principle of the superconductivity technology to measure weak forces is that when the relative position between the superconductor and coil changes, the inductance of the system will change; therefore, we obtained the position change of the superconductor, which was used to measure the weak force and reached the order of 10^{-10} N. Optical tweezers use optical radiation to capture particles in the center of the optical trapping. When subjected to other weak disturbances, particles deviate from the center of the optical trap; therefore, we obtained the displacement information of the particles, which was used for the weak-force measurement, and could currently reach 10^{-15} N magnitude [6]. Optical tweezers possess the advantages of noncontact manipulation and no damage, thereby greatly improving the accuracy of weak-force measurements. They are used in cell biology, such as cell surgery with laser scalpels [7] and cell fusion manipulation [8, 9], cell membrane elasticity measurements [10, 11], and chromosome motion studies [12, 13]. In addition, they are used to produce accelerometers [14]. Recently, the optical-tweezer technology has been rapidly developed into a variety of special optical tweezers, such as holographic [15–17], time-sharing scanning [18, 19], and fiber optical tweezers [20–22]. The application prospects of optical tweezers are immeasurable. For these applications, the detection sensitivity is a key factor affecting information extraction and application.

The sensitivity of optical tweezers requires improvement to achieve the high precision of weak-force measurements. Presently, the sensitivity measurement of optical tweezers generally adopts the sensitivity calculation formula obtained from the minimum detectable force (MDF) [23] formula: $S_{\min} = F_{\min} / f = \sqrt{4 \ k_B T \ _0}$. However, the system parameters, such as the environment temperature, particle radius, and density of the actual values, typically deviate from the theoretical values, and the sensitivity obtained by fitting using the theoretical values of different parameters deviates from the actual value. Here, a method for measuring the sensitivity of a system using a Coulomb force is proposed. We applied the appropriate magnitude of the Coulomb force in the experiment, changed the resolution bandwidth to render SNR (signal-to-noise ratio) = 1, and obtained the system sensitivity as $1.827\ 5\times10^{-17}$ N/Hz$^{1/2}$. Compared with a reported indirect-measurement method, the proposed method was a direct-measurement method that did not require the accurate determination of the deviation between the actual and theoretical values of the system parameters and other noise sources in advance, and its result was more accurate. To select the appropriate range of the Coulomb force and bandwidth, we used Simulink to establish a simulation model.

Sensitivity is mainly the restriction of optical-tweezer application in the Casimir force measurements and non-Newtonian gravity model verification. In vacuum optical tweezers, the determination of the sensing sensitivity and SNR is important for evaluating the force detection ability of optical tweezers. The existing sensitivity measurement method is mainly through particle diameter fitting and other methods to obtain the parameters, calculate the damping coefficient, and obtain the theoretical sensitivity. In the vicinity of the resonant peak, the thermal noise dominates. Thus, this method is feasible, but technical errors remain, such as the error of fitting parameters. When the frequency is far from the resonant peak, other noises such as the electrical noise require consideration. Thus, the existing method for

measuring sensitivity is inaccurate.

According to the definition of the sensitivity, when SNR = 1, the corresponding signal can be regarded as the MDF in the system, and the system sensitivity can be obtained by considering the analysis bandwidth. Here, a force with the controllable frequency and amplitude was applied to the system using the electrostatic force as the input. Using different analysis bandwidths, the SNR, sensitivity, and resolution of the system at different inputs and frequencies were directly evaluated. This method used the external force as the input, directly evaluated the measurement parameters of the system, and directly studied the system noise and weak signal measurement situations, particularly under high vacuum conditions.

Firstly, we introduce the principle of the proposed method, established simulation model, and experiment. Thereafter, we present the simulation model and composition of the experimental device. Finally, we discuss the simulation and experimental results.

2. Principle and methods

2.1 Particle motion equation and SNR of displacement detection

The particle motion equation in optical tweezers can be theoretically expressed as

$$M\frac{\mathrm{d}^2x}{\mathrm{d}t^2}+\gamma\frac{\mathrm{d}x}{\mathrm{d}t}+\kappa x=F_{\mathrm{therm}}(t) \tag{1}$$

where M, γ, and F_{therm} correspond to the particle mass, Stokes friction coefficient, and thermal force, respectively. They are related to the temperature T, particle radius R, and ambient pressure P with the following relationship:

$$\begin{aligned}\gamma&=6\pi\eta R\\ F_{\mathrm{therm}}(t)&=2k_BT\gamma\xi(t)\end{aligned} \tag{2}$$

where $\xi(t)$ is the normalized white noise process.

If an external force excitation, F_{in}, is applied to the particle in the optical tweezers, the particle motion equation can be expressed as

$$M\frac{\mathrm{d}^2x}{\mathrm{d}t^2}+\gamma\frac{\mathrm{d}x}{\mathrm{d}t}+\kappa x=F_{\mathrm{therm}}(t)+F_{\mathrm{in}}. \tag{3}$$

Assuming that the power spectrum of F_{in} is $F(\omega)$, the power spectrum density of the particle displacement can be obtained using the following equation:

$$\begin{aligned}S(\omega)&=\frac{2k_BT\Gamma_0}{M(\Omega^2-\omega^2)^2+\omega^2\Gamma_0^{\ 2}}+\frac{F(\omega)}{M(\Omega^2-\omega^2)^2+\omega^2\Gamma_0^{\ 2}}\\&=A+B\end{aligned} \tag{4}$$

where ω is the resonant frequency of the particles, k_B is the Boltzmann constant, and Γ_0 is the damping coefficient. $A=\frac{2k_BT\Gamma_0}{M(\Omega^2-\omega^2)^2+\omega^2\ \Gamma_0^{\ 2}}$, denoting the power spectral density of the noise, which is mainly the thermal noise. $B=\frac{F(\omega)}{M(\Omega^2-\omega^2)^2+\omega^2\ \Gamma_0^{\ 2}}$, representing the signal power spectral density. Considering a certain analysis bandwidth, f_{BW} and $f_{\mathrm{BW}}\ll\omega/2\pi$, SNR can be expressed as

$$\mathrm{SNR}=\frac{S}{N\sqrt{f_{\mathrm{BW}}}}. \tag{5}$$

According to (5), we obtain

$$\mathrm{SNR}^2=\frac{B}{Af_{\mathrm{BW}}}=\frac{F(\omega)}{2k_BT\Gamma_0f_{\mathrm{BW}}}=\frac{F_{\mathrm{in}_0}^2}{4\pi k_BT\Gamma_0f_{\mathrm{BW}}} \tag{6}$$

where F_{in_0} is the amplitude of the input Coulomb force.

When SNR = 1, F_{in_0} is the MDF. F_{min} can be obtained as

$$F_{\mathrm{min}}=\sqrt{4\pi k_BT\Gamma_0f_{\mathrm{BW}}}. \tag{7}$$

By lowering the harmonic oscillator temperature T and damping coefficient Γ_0, the amplitude of the MDF can be reduced, such that the sensitivity is increased, and the detection ability can be improved. However, here, the particle was in a low-vacuum environment. Therefore, the dissipative mechanism of the particle and the cooling device of the vacuum optical-tweezer system were sufficient to maintain the ambient temperature. Thus, the particle was in the thermal equilibrium, and we did not need to consider the relationship between the temperature

and sensitivity. By considering the measurement bandwidth, the theoretical sensitivity of the system was obtained as follows:

$$S_{\min} = \frac{F_{\min}}{\sqrt{f_{\mathrm{BW}}}} = \sqrt{4\pi k_B T \Gamma_0}\ . \tag{8}$$

According to (6) and (7), the following inferences can be made:

1. SNR is proportional to the amplitude of the input signal.

2. The minimum detectable signal is related to the 1/2 power of the analysis bandwidth, f_{BW}.

Experimental systems, in addition to the thermal noise, typically included the electronic noise, and system parameters, such as the particle radius and environmental pressure, slightly deviated from the theoretical values, which we thought other noise factors that could cause the actual sensitivity to disagree with the theoretical sensitivity. Assuming that the other noise power spectrum density is $C = \dfrac{C_0}{M(\Omega^2 - \omega^2)^2 + \omega^2\ \Gamma_0^2}$, where C_0 is a constant corresponding to the broadband white noise, we obtain

$$\begin{aligned} \mathrm{SNR}^2 &= \frac{B}{(A+C)f_{\mathrm{BW}}} = \frac{F(\omega)}{(2k_B T\Gamma_0 + C_0)f_{\mathrm{BW}}} \\ &= \frac{F_{\mathrm{in}_0}^2}{2\pi f_{\mathrm{BW}}(2k_B T\Gamma_0 + C_0)}. \end{aligned} \tag{9}$$

When SNR = 1, F_{in_0} is the MDF, which can be obtained as

$$F'_{\min} = \sqrt{(4\pi k_B T\Gamma_0 + 2\pi C_0)f_{\mathrm{BW}}}\ . \tag{10}$$

The actual sensitivity of the system can be expressed as

$$S'_{\min} = \frac{F'_{\min}}{\sqrt{f_{\mathrm{BW}}}} = \sqrt{4\pi k_B T\Gamma_0 + 2\pi C_0} = S_{\min}\sqrt{1 + \frac{2\pi C_0}{S_{\min}^2}}\ . \tag{11}$$

When ω is close to the resonant frequency, $\dfrac{2\pi C_0}{S_{\min}^2} \ll 1$, such that $S'_{\min} \approx S_{\min}$, but when ω is far from the resonant frequency, $\dfrac{2\pi C_0}{S_{\min}^2} \geq 1$; therefore, $S'_{\min} \neq S_{\min}$. We can obtain the magnitude of C_0 using (11).

2.2 Generation of input excitation weak force

The suspended particles in the vacuum optical tweezers typically possess a certain charge in the loading process, and the specific charge, q, can be experimentally measured and controlled. Its typical value ranges from several to dozens of electrons, and the amount of the charge can be regulated by ionization [24].

If the voltage, $U = U_0 \sin(2\pi f_0 t)$, is applied to the captured region at this time, a force related to the voltage can be applied to the particle:

$$F_{\mathrm{in}} = qE = KqU_0 \sin(2\pi f_0 t) \tag{12}$$

where K was obtained as 350 after the electric field calibration, q is the charge amount carried by the particles, E is the electric field intensity, U_0 is the voltage amplitude, and f_0 is the frequency of the applied voltage. F_{in} was proportional to U, with the same frequency and phase, and we changed the magnitude and frequency of the force by changing the magnitude and frequency of U. In particular, if $f_0 = 0$, the static input was provided for the particles. The possible force applied was calculated by (12) (Fig. 1). For example, when $q = 50e$, $U_0 = 250$ V, the amplitude of the force that could be applied was 7.14×10^{-13} N. For $q = 1e$, $U_0 = 1$ μV, the applied force amplitude was 5.72×10^{-23} N. This force can be used in a wide range of applications (Fig.1).

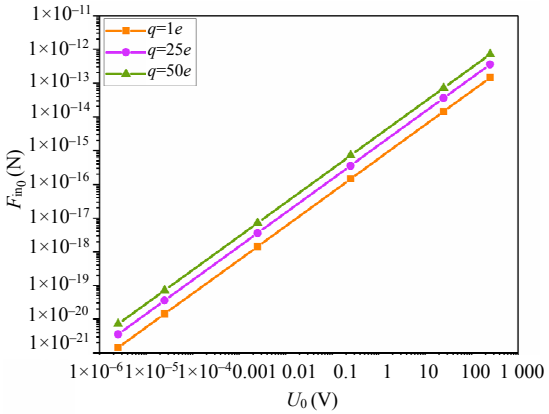

Fig. 1 Relationship between F_{in_0} and U_0 (logarithmic coordinate system).

3. Simulation model and experimental setup

The simulation flow chart is shown in Fig. 2, which was modeled using Simulink to realize the process. Firstly, we input external, random, damping, and optical trapping forces. Thereafter, we processed through the addition, product, and integrator functions. Finally, we calculated the particle displacement information through the simulation model. The core of this simulation model is the second-order differential equation, namely the Langevin equation of micro/nanoparticle motion, which is expressed as (3). The pink parallelogram represents the different forms of the applied Coulomb force.

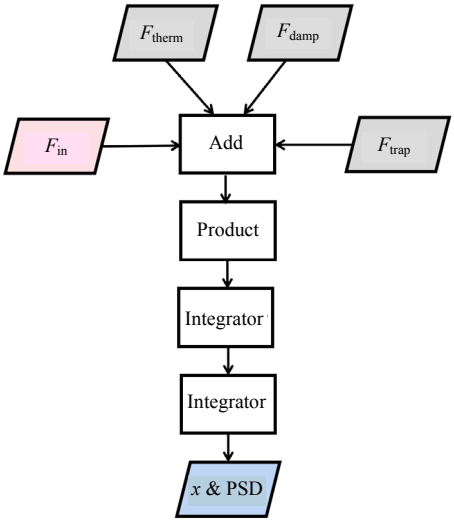

Fig. 2 Simulation flow chart.

Figure 3 shows a schematic diagram of the experimental device (P = 1 mbar). A 1064-nm laser with a trapping power of 180 mW was used to form optical tweezers at the focal point through the focusing lens and optical trapping stiffness, κ = 3.659×10^{-6} N/m, obtained using the Zurich Instruments (ZI) graphical user interface particle calibration software of the Zhejiang Laboratory. The test particles were silica particles with a radius of 80 nm, which were loaded through the atomizer and captured by optical trapping. The forward-scattered light of the particles passed through a D-shaped mirror, and a balanced photodetector was used to extract the movement information of the particles. A bare electrode was placed approximately 1 cm away from the center of the optical trap, and a high voltage (HV) of approximately 3 kV was applied to ionize the air for charge control. The amplitude of the electric drive response signal of the particle was obtained using a ZI phase lock, and the amplitude of the voltage of a single electron was obtained to determine the amount of charges carried by the particle. An electric field was provided in the capturing region through the front and back plate electrodes, and a force input was applied to the charged silica particles by changing the applied voltage amplitude and frequency. Figure 4 illustrates the particle whose charge is 50e in an electric field when a sinusoidal voltage is applied. The charged particle was affected by the Coulomb force, F_{in}, and deviated from the center of the optical trapping. Thus, the optical tweezers generated an optical trapping force, $F_{opt} = \kappa x$, on the particle to balance with the Coulomb force, such that the particle did not escape from the capture area but only moved within it. Its time-domain motion curve was “beat” (Fig. 4).

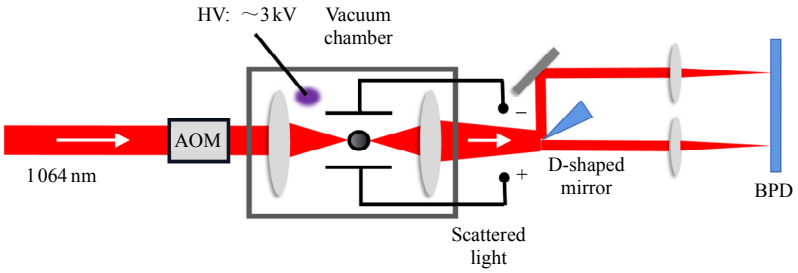

Fig. 3 Schematic diagram of the experimental device.

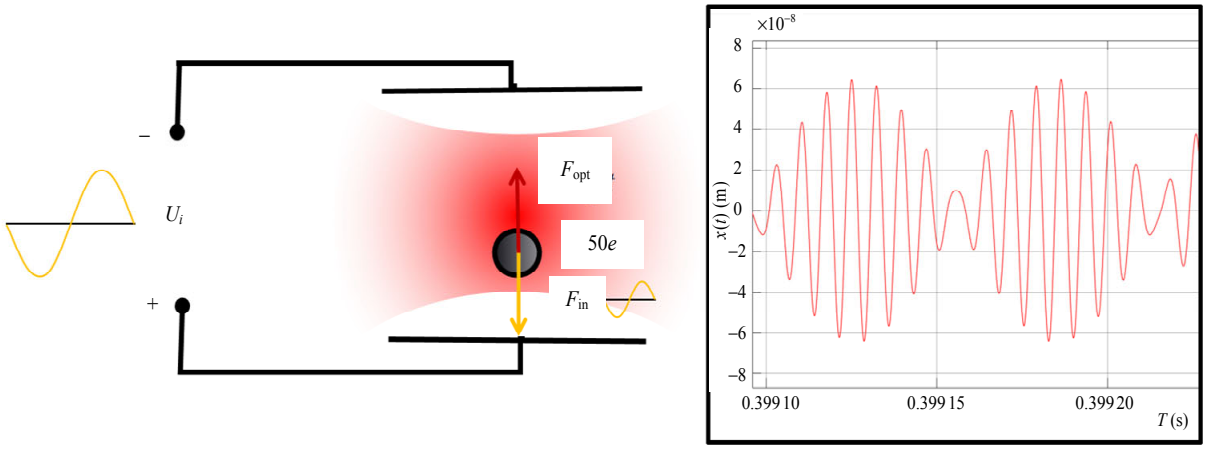

Fig. 4 Charged particle and electric field in the capturing region.

4. Results and discussion

4.1 Verification of the correctness of the simulation model

According to the information provided by the producer, T = 300 K, P = 2.5×10^{-4} mbar, R = 80 nm, and the particle density ρ = 2.0 g/cm^3. Through air ionization [24], we determined that the charge of the silica particle was 50e, the resonant frequency of the particle was 147 kHz, κ = 3.659×10^{-6} N/m, and the applied voltage was $U = 12\sin(130k \times 2\pi \times t)$ between the positive and negative electrodes. The simulation results are shown in Fig. 5(a), $x(t)$(m) in the vertical axis similar to that in the figures below indicated the particle displacement, whose unit was the meter. The "beat" of the low-frequency amplitude variation, whose frequency was 17 kHz, was equal to the frequency difference between 147 kHz and 130 kHz, correlated with the theoretical prediction. The experimental results are shown in Fig. 5(b), and the "beat" was observed. The calculated experimental beat frequency was 16.92 kHz, with an error of 0.47% from the simulation result, which was within the acceptable range.

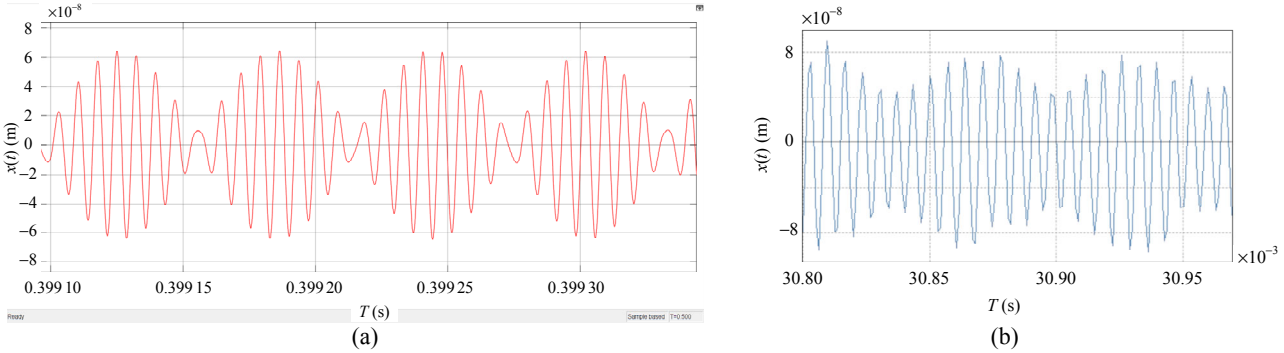

Fig. 5 "Beat" generated by applying the sinusoidal Coulomb force: (a) simulation and (b) experimental results.

Next, we maintained the experimental conditions as above and applied a fixed voltage, $U_0 = 220$ V, to provide a step Coulomb force to the particle at t = 0.7 s, whose theoretical value was calculated as $F_{the} = qE = 5.815\ 2 \times 10^{-13}$ N. Figure 6(a) shows the simulation results. A descending "step" phenomenon was observed, whose height Δx_{sim} was 159.05 nm. The Coulomb force in the simulation was $F_{sim} = \kappa \Delta x_{sim} = 5.819\ 6 \times 10^{-13}$ N, 0.076% from the theoretical value and was negligible. The experimental results are shown in Fig. 6(b), and a descending "step" was also observed. The height of the "step" was obtained through data processing as $\Delta x_{exp} = 142.31$ nm, and the error

between the experimental Coulomb force, $F_{\mathrm{exp}} = \kappa \Delta x_{\mathrm{exp}} = 5.207\ 1 \times 10^{-13}$ N , and theoretical Coulomb force was 10.5%, which was within the acceptable range because of the accuracy of κ and other noise sources.

These results confirmed the correctness of the simulation model.

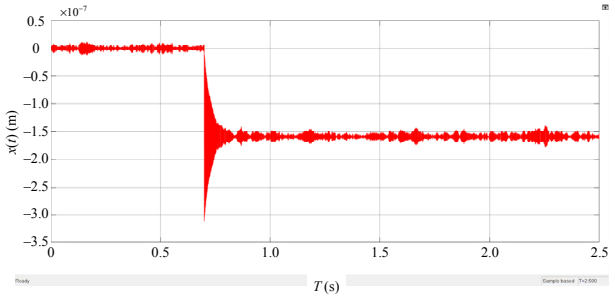

(a)

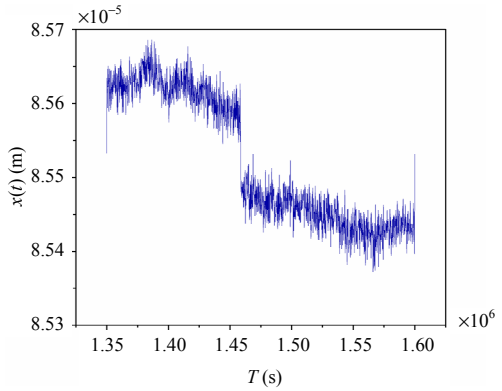

(b)

Fig. 6 "Step" generated by applying the step Coulomb force: (a) simulation and (b) experimental results.

4.2 Simulation calibration

The analysis bandwidth was set to 1 Hz, and a sinusoidal Coulomb force with a frequency of 140 kHz was applied to the particle. During the simulation, the amplitude of the Coulomb force, F_{in}, varied from F_{min} to $90F_{\mathrm{min}}$, and the corresponding SNRs were measured (Fig. 7). The black curve represents the theoretical calculation results, and the blue curve represents the simulation results. Within the applied Coulomb force range, the experimental results were correlated with the theoretically calculated values. Both results linearly changed with the applied Coulomb force.

Afterward, we applied a 140-kHz sinusoidal Coulomb force with a fixed amplitude of $5F_{\mathrm{min}}$ to the particle and changed the analysis bandwidth in the range of 0.01 Hz – 5 Hz. The corresponding SNRs are shown in Fig. 8 in logarithmic coordinates. The black square curve represents the theoretical calculation results, and the blue curve represents the simulation results. Within the measured analysis bandwidth range, the experimental result was greatly correlated with the theoretical calculation result, and both results linearly changed in the logarithmic coordinate system. As the analysis bandwidth decreased, SNR increased. This calibration process provided a reference for the range selection of the Coulomb force and analysis bandwidth for this experiment.

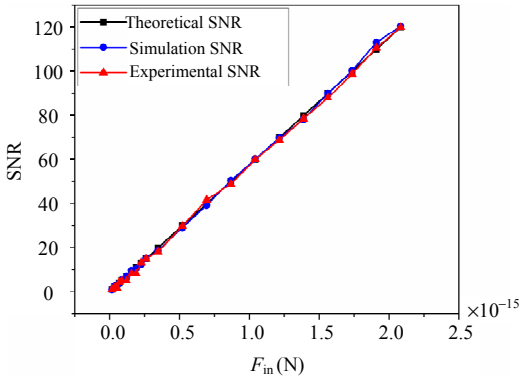

Fig. 7 Relationship between SNR and F_{in_0} .

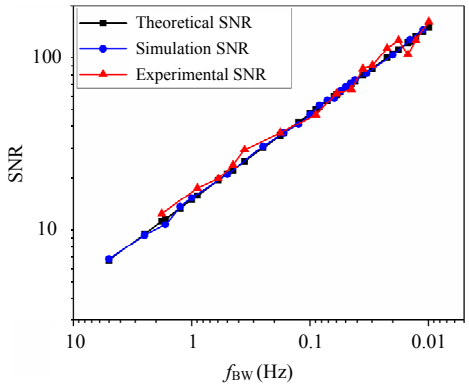

Fig. 8 Relationship between SNR and f_{BW} .

4.3 Experimental results

According to the simulation results, during the experiment, the analysis bandwidth was set to 1 Hz, and the amplitude range of F_{in} was F_{min} – $120F_{\mathrm{min}}$ by

adjusting the amplitude of the applied voltage. The experimental results are shown in Fig. 7, and the conclusions were correlated with the simulation results. Figure 9 shows two parts of the power spectral density curve in the experiment by the Fourier transform analysis of the particle displacement curve. We collected 10 groups of time-domain data in the same experiment and obtained 10 groups of frequency-domain data by the Fourier transform analysis using MATLAB. The final frequency-domain curve (Fig. 9) was obtained by averaging. The yellow triangle indicates the signal peak generated by applying an electric field. When $F_{in_0} = F_{min}$, the magnitude of the signal was close to that of noise, and when $F_{in_0} = 9F_{min}$, the signal magnitude was approximately nine times that of noise, which was correlated with the simulation results. When the SNR and analysis bandwidth are known, we can determine the magnitude of the external force on the particle according to the relationship between the SNR and applied external force. As shown in Fig. 7, when SNR = 1, the actual MDF, $F'_{min} = 1.827\ 5\times10^{-17}$ N; therefore, the actual measured sensitivity, $S'_{min} = 1.827\ 5\times10^{-17}$ N / Hz$^{1/2}$ can be substituted into (11) to obtain the power spectral density of other noises.

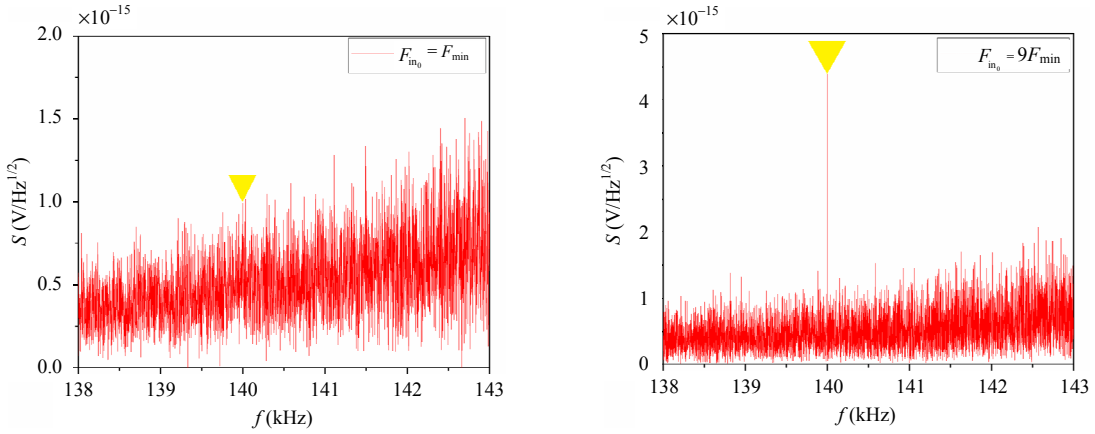

Fig. 9 Power spectral density curve when f_{BW} is constant: (a) $F_{in_0} = F_{min}$ and (b) $F_{in_0} = 9F_{min}$.

Subsequently, the amplitude of the applied Coulomb force was set to $15F_{min}$, and the analysis bandwidth range was 0.01 Hz – 1.788 1 Hz. The experimental results are shown in Fig. 8. The black curve represents the theoretical results within the analysis bandwidth range, and the red curve represents the experimental results, which linearly changed in the logarithmic coordinate system.

4. Conclusions

Herein, we proposed a novel method whose measurement precision and uncertainty were 5.3% and 6.2%, respectively, for measuring the system sensitivity using a Coulomb force. The actual sensitivity of the optical-tweezer system was obtained by applying the appropriate magnitude of the Coulomb force to render SNR = 1. Compared with the theoretical sensitivity, we obtained the magnitude of other noises in the experimental system. In addition, we confirmed the validity of the proposed method.

Firstly, a simulation model of micro/nanoparticle dynamics in the optical-tweezer system was established using Simulink, and the correctness of the simulation model was experimentally verified. In this model, the relationship among SNR, f_{BW}, and F_{in} was obtained by applying a Coulomb force and changing the analysis bandwidth to complete the calibration process, which provided a reference for the range selection of the Coulomb force and analysis bandwidth in such experiments. Next, we set the Coulomb forces and analysis bandwidths in

the experimental system to a suitable range. When SNR = 1, the actual sensitivity of the system was measured to be 1.8275×10^{-17} N/Hz$^{1/2}$.

Compared with the indirect method that uses the formula to calculate and fit, this proposed method is a direct method for obtaining the actual sensitivity of any optical-tweezer system as long as the trapped particles are charged. It is also possible to determine the difference between the actual and theoretical values of the system parameters and other noise sources in advance. Thus, we can indirectly calculate the magnitude of other noises, which can improve the performance of the optical-tweezer system to its theoretical limit.

Acknowledgment

The research was supported by the National Natural Science Foundation of China (Grant Nos. 62075193, 11304282, and 61601405), Joint Fund of Ministry of Education, China (Grant No. 6141A02011604), Major Scientific Research Project of Zhejiang Lab, China (Grant No. 2019MB0AD01), National Program for Special Support of Top-Notch Young Professionals, China (Grant No. W02070390), and Fundamental Research Funds for the Central Universities, China (Grant Nos. 2016XZZX004-01 and 2018XZZX001-08).

References

[1] R. D. Newman and M. K. Bantel, “On determining Gusing a cryogenic torsion pendulum,” *Measurement Science and Technology*, 1999, 10(6): 445.

[2] N. A. Chaturvedi, T. Lee, M. Leok, and N. H. McClamroch, “Nonlinear dynamics of the 3D pendulum,” *Journal of Nonlinear Science*, 2011, 21: 3–32.

[3] G. B. Walker and D. G. Lahoz, “Experimental observation of Abraham force in a dielectric,” *Nature*, 1975, 253(5490): 339–340.

[4] G. L. Klimchitskaya and V. M. Mostepanenko, “Experiment and theory in the Casimir effect,” *Contemporary Physics*, 2006, 47(3): 131–144.

[5] K. A. Polzin, T. E. Markusic, B. J. Stanojev, A. Dehoyos, and B. Spaun, “Thrust stand for electric propulsion performance evaluation,” *Review of Scientific Instruments*, 2006, 77(10): 105108.

[6] G. Ranjit, M. Cunningham, K. Casey, and A. A. Geract, “Zeptonewton force sensing with nanospheres in an optical lattice,” *Physical Review A*, 2016, 93(5): 053801.

[7] J. R. Aist, H. Liang, and M. W. Berns, “Astral and spindle forces in PtK2 cells during anaphase B: a laser microbeam study,” *Journal of Cell Scienc*e, 1993, 104(Pt 4): 1207–1216.

[8] M. M. Burns, J. M. Fournier, and J. A. Golovchenko, “Optical matter: crystallization and binding in intense optical fields,” *Science*, 1990, 249(4970): 749–754.

[9] R. W. Steubing, S. Cheng, W. H. Wright, Y. Numajiri, and M. W. Berns, “Laser induced cell fusion in combination with optical tweezers: the laser cell fusion trap,” *Cytometry*, 2010, 12(6): 505–510.

[10] S, M. Block, “Kinesin motor mechanics: binding, stepping, tracking, gating, and limping,” *Biophysical Journal*, 2007, 92(9): 2986–2995.

[11] Y. Okada and N. Hirokawa, “A processive single-headed motor: kinesin superfamily protein KIF1A,” *Science*, 1999, 283(5405): 1152–1157.

[12] M. W. Berns, W. H. Wright, B. J. Tromberg, and R. J. Walter, “Use of a laser-induced optical force trap to study chromosome movement on the mitotic spindle,” *Proceedings of the National Academy of Sciences of the United States of America*, 1989, 86(12): 4539–4543.

[13] R. B. Nicklas, “Measurements of the force produced by the mitotic spindle in anaphase,” *The Journal of Cell Biology*, 1983, 97(2): 542–548.

[14] L. Feng, H. Jiao, and B. Yao, “Sensitivity analysis of light force accelerometer based on optical trapping Mie microsphere,” *Optoelectronics Letters*, 2014, 10(1): 77–80.

[15] E. R. Dufresne and D. G. Grier, “Optical tweezer arrays and optical substrates created with diffractive optics,” *Review of Scientific Instruments*, 1998, 69(5): 1974–1977.

[16] D. R. Burnham and D. Mcgloin, “Holographic optical trapping of aerosol droplets,” *Optics Express*, 2006, 14(9): 4176–4182.

[17] B. Sun, Y. Roichman, and D. G. Grier, “Theory of holographic optical trapping,” *Optics Express*, 2008(16): 15765–15776.

[18] J. G. Wu, Y. X. Ren, Z. Q. Wang, C. Zhou, and Y. M.

Li, "Time-sharing multiple optical traps using rotating glass plate," *Chinese Journal of Lasers*, 2009, 36(10): 2751–2756.

[19] L. Yuan, Z. H. Liu, J. Yang, and C. Y. Guan, "Twin-core fiber optical tweezers," *Optics Express*, 2008, 16(7): 4559–4559.

[20] R. R. Ribeiro, O. Soppera, A. G. Oliva, A. Guerreiro, and P. S. Jorge, "New trends on optical fiber tweezers," *Journal of Lightwave Technology*, 2015, 33(16): 3394–3405.

[21] J. Huisstede, B. Rooijen, K. Werf, M. Bennink, and V. Subramaniam, "Dependence of silicon position-detector bandwidth on wavelength, power, and bias," *Optics Letters*, 2006, 31(5): 610–612.

[22] A. Farré, F. Marsà, and M. Montes-Usategui, "Optimized back-focal-plane interferometry directly measures forces of optically trapped particles," *Optics Express*, 2012, 20(11): 12270.

[23] S. Kuehn, S. A. Hickman, and J. A. Marohn, "Advances in mechanical detection of magnetic resonance," *Journal of Chemical Physics*, 2008, 128: 052208.

[24] M. Frimmer, K. Luszcz, S. Ferreiro, V. Jain, E. Hebestreit, and L. Novotny, "Controlling the net charge on a nanoparticle optically levitated in vacuum," *Physical Review A*, 2017, 95(6): 061801.